

Bridging the Usability Gap: Theoretical and Methodological Advances for Spectral Learning of Hidden Markov Models

Xiaoyuan Ma

Department of Statistics, University of Virginia
and

Jordan Rodu

Department of Statistics, University of Virginia

February 16, 2023

Abstract

The Baum-Welch (B-W) algorithm is the most widely accepted method for inferring hidden Markov models (HMM). However, it is prone to getting stuck in local optima, and can be too slow for many real-time applications. Spectral learning of HMMs (SHMMs), based on the method of moments (MOM) has been proposed in the literature to overcome these obstacles. Despite its promises, asymptotic theory for SHMM has been elusive, and the long-run performance of SHMM can degrade due to unchecked propagation of error. In this paper, we (1) provide an asymptotic distribution for the approximate error of the likelihood estimated by SHMM, and (2) propose a novel algorithm called projected SHMM (PSHMM) that mitigates the problem of error propagation, and (3) develop online learning variations of both SHMM and PSHMM that accommodate potential nonstationarity. We compare the performance of SHMM with PSHMM and estimation through the B-W algorithm on both simulated data and data from real world applications, and find that PSHMM not only retains the computational advantages of SHMM, but also provides more robust estimation and forecasting.

Keywords: hidden Markov models (HMM), spectral estimation, projection-onto-simplex, online learning, time series forecasting

1 Introduction

Hidden Markov model (HMM) (Baum and Petrie, 1966) is a widespread model with applications in many areas, such as finance, natural language processing and biology. An HMM is a stochastic

probabilistic model for sequential or time series data that assumes that the underlying dynamics of the data are governed by a Markov chain. (Knoll et al., 2016).

The Baum-Welch algorithm (Baum et al., 1970), which is a special case of expectation–maximization (EM) algorithm (Dempster et al., 1977) based on maximum likelihood estimation (MLE), is a popular approach for inferring the parameters of the HMM. However, the EM algorithm requires large number of iterations until the parameter estimates converge—which has a large computational cost, especially for large-scale time series data—and can easily get trapped in local optima. In order to overcome these issues especially for large, high dimensional time series, Hsu et al. (2012) proposed a spectral learning, i.e. method of moments (MOM), algorithm for HMMs (SHMM) with attractive theoretical properties. However, the finite sample size behavior of the algorithm was not well-characterized. Later, Rodu (2014) improved the spectral estimation algorithm and extended it to HMMs with high-dimensional and continuously-distributed output, but again did not address finite sample properties. In this manuscript, we provide a theoretical discussion of the finite sample behavior of SHMM algorithms.

In addition to providing theorems related to the finite sample behavior of SHMMs, we provide a novel improvement to the SHMM family of algorithms. Our improvement is motivated from an extensive simulation study of the methods proposed in Hsu et al. (2012) and Rodu (2014). We found that spectral estimation does not provide stable results under the low signal-noise ratio setting. We propose a new spectral estimation method, the projected SHMM (PSHMM), that leverages a novel regularization technique that we call ‘projection-onto-simplex’ regularization. The PSHMM largely retains the computational advantages of SHMM methods without sacrificing accuracy.

In addition to proposing the PSHMM, we provide a novel extension of spectral estimation (including all SHMM and PSHMM approaches) to allow for online learning. We propose two approaches – the first speeds up computational speed for learning a model in large data settings, and the second incorporates “forgetfulness” which allows for adapting to changing dynamics of the data. This speed and flexibility is crucial, for instance, in high frequency trading, and we show the effectiveness of the PSHMM on real data in this setting.

The structure of this paper is as follows: In the rest of this section, we will introduce existing models. In Section 2, we provide theorems on the finite sample properties of SHMMs. Section 3

introduces our new method, PSHMM. In Section 4, we extend the spectral estimation to online learning for both SHMM and PSHMM. Then, section 5 shows the simulation results and Section 6 shows the application on high frequency trading. We will have a deep discussion in Section 7.

1.1 The hidden Markov model

The standard HMM (Baum and Petrie, 1966) is defined by a set of S hidden categorical states $1, 2, \dots, S$ that evolve according to a Markov chain. We denote the hidden state at time t as h_t . The Markov chain is characterized by an initial probability $\pi_0 = [\pi_0^{(1)}, \dots, \pi_0^{(S)}]$ where $h_1 \sim \text{Multinomial}(\pi_0^{(1)}, \dots, \pi_0^{(S)})$, and a transition matrix $\mathbf{T} = [\mathbf{T}_{ij}]_{i=1, \dots, S}^{j=1, \dots, S}$ where $\mathbf{T}_{ij} = P(h_{t+1} = j | h_t = i)$ for $\forall t$. The emitted observation X_t is distributed conditional on the value of the hidden state at time t , $X_t | h_t = s \sim \mathcal{F}_s$ where \mathcal{F}_s is the emission distribution conditioned on the hidden state $h_t = s$. The standard HMM's parameters are $(\pi_0, \mathbf{T}, \{\mathcal{F}_s\}_{s=1}^S)$. Figure 1 is a graphical representation of the standard HMM. Typically, if the emission follows a Gaussian distribution, then we call it Gaussian HMM (GHMM).

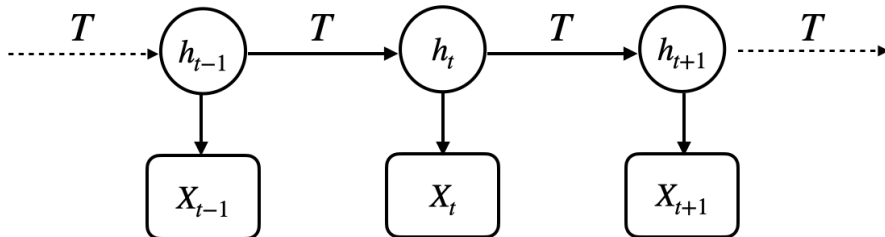


Figure 1: Model structure of standard HMM. $\{h_t\}$ is a latent Markov chain evolves according to transition matrix \mathbf{T} . For each time stamp t , the observed X_t is generated according to the emission distribution associated with h_t .

1.2 Spectral learning of HMM

The model proposed by Rodu (2014) is shown in Figure 2. Again, h_t denotes the hidden state at time t , and X_t the emitted observation. For estimation of the model, these observations are further projected onto a lower dimensional space of dimensionality d and the lower dimensional

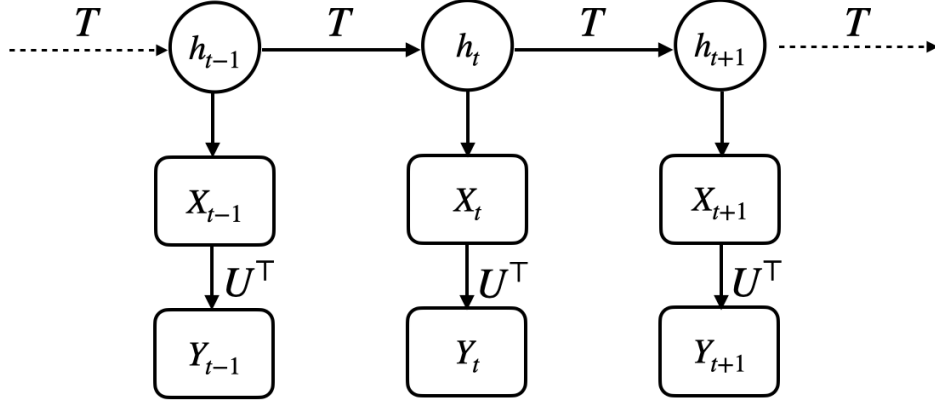


Figure 2: Spectral estimation model by Rodu (2014). Besides the latent state series $\{h_t\}_t$ and observed series $\{X_t\}_t$, Rodu (2014) introduced a reduced-dimensional series $\{Y_t = U^\top X_t\}$ which is a projection of X_t on a lower-dimensional subspace whose dimensionality is equal to the number of hidden states. Then the spectral estimation will be performed based on $\{Y_t\}_t$.

observations are denoted $y_t = U^\top x_t$. We discuss the choice of dimension d and the projection of the observations in Section 3.3.

Using the spectral estimation framework, the likelihood can be written as:

$$Pr(x_{1:t}) = c_\infty^\top C(y_t)C(y_{t-1}) \cdots C(y_1)c_1, \quad (1)$$

where

$$\begin{aligned} c_1 &= \mu, c_\infty^\top = \mu^\top \Sigma^{-1}, C(y) = K(y)\Sigma^{-1}, \\ \mu &= E(y_1) = U^\top M\pi, \\ \Sigma &= E(y_2 y_1^\top) = U^\top M T \text{diag}(\pi) M^\top U, \\ K(a) &= E(y_3 y_1^\top y_2^\top) a = U^\top M T \text{diag}(M^\top U a) T \text{diag}(\pi) (M^\top U), \\ M &= [M_1, \cdots, M_S] \text{ where } M_i = E(X|i). \end{aligned}$$

These quantities can be empirically estimated as:

$$\hat{Pr}(x_{1:t}) = \hat{c}_\infty^\top \hat{C}(y_t) \hat{C}(y_{t-1}) \cdots \hat{C}(y_1) \hat{c}_1, \quad (2)$$

where

$$\begin{aligned}\hat{c}_1 &= \hat{\mu}, \hat{c}_\infty^\top = \hat{\mu}^\top \hat{\Sigma}^{-1}, \hat{C}(y) = \hat{K}(y) \hat{\Sigma}^{-1}, \\ \hat{\mu} &= \frac{1}{N} \sum_{i=1}^N Y_i, \\ \hat{\Sigma} &= \frac{1}{N} \sum_{i=1}^{N-1} Y_{i+1} Y_i^\top, \\ \hat{K}(y) &= \frac{1}{N} \sum_{i=1}^{N-2} Y_{i+2} Y_i^\top \cdot Y_{i+1}^\top y.\end{aligned}$$

Prediction of y_t is computed recursively by:

$$\hat{y}_t = \frac{C(y_{t-1}) \hat{y}_{t-1}}{c_\infty^\top C(y_{t-1}) \hat{y}_{t-1}}; \quad (3)$$

Observation x_t can be recovered as:

$$\hat{x}_t | x_1, x_2, \dots, x_{t-1} = U \hat{y}_t. \quad (4)$$

See Rodu et al. (2013) for detailed derivations and mathematical proof of these results.

2 Theoretical Properties of SHMM

In general, SHMM estimates the likelihood through the MOM. Although MOM gives fast approximation, the theoretical properties of SHMM estimation are less well studied. Hsu et al. (2012) and Rodu et al. (2013) give the conditions where the spectral estimator converges to the true likelihood almost surely:

$$\hat{P}r(x_{1:T}) = \hat{c}_\infty^\top \hat{C}(y_t) \hat{C}(y_{t-1}) \cdots \hat{C}(y_1) \hat{c}_1 \xrightarrow{a.s.} Pr(x_{1:T}), \quad (5)$$

In this manuscript, we study the asymptotic distribution of $\hat{P}r(x_{1:T}) - Pr(x_{1:T})$. Theorem 1 shows a central limit theorem type bound of the approximation error. First, however, we identify the sources of error for the SHMM in the following lemma.

Lemma 1.

$$\hat{P}r(x_{1:T}) = Pr(x_{1:T}) + (v + \tilde{v})^\top \widehat{\Delta\mu} + \sum_{t=1}^T a_t^\top \widehat{\Delta K}(y_t) \tilde{a}_t - \sum_{t=0}^T b_t^\top \widehat{\Delta\Sigma} \tilde{b}_t + O_p(N^{-1}),$$

where

$$\begin{aligned}
v &= (\mu^\top \Sigma^{-1} K(y_T) \cdots K(y_1) \Sigma^{-1})^\top; & \tilde{v} &= \Sigma^{-1} K(y_T) \cdots K(y_1) \Sigma^{-1} \mu; \\
a_t &= (\mu^\top \Sigma^{-1} K(y_T) \Sigma^{-1} \cdots K(y_{t+1}) \Sigma^{-1})^\top; & \tilde{a}_t &= \Sigma^{-1} K(y_{t-1}) \cdots K(y_1) \Sigma^{-1} \mu; \\
b_t &= (\mu^\top \Sigma^{-1} K(y_T) \Sigma^{-1} \cdots \Sigma^{-1} K(y_{t+1}) \Sigma^{-1})^\top; & \tilde{b}_t &= \Sigma^{-1} K(y_t) \Sigma^{-1} \cdots K(y_1) \Sigma^{-1} \mu.
\end{aligned}$$

Proof (Lemma 1). *First, we expand the estimated likelihood by decomposing it into the underlying truth and the error terms. We have*

$$\begin{aligned}
& \widehat{Pr}(x_{1:T}) \\
&= \hat{c}_\infty^\top \hat{C}(y_T) \hat{C}(y_{T-1}) \cdots \hat{C}(y_1) \hat{c}_1 \\
&= (\hat{\mu}^\top \hat{\Sigma}^{-1}) [\hat{K}(y_T) \hat{\Sigma}^{-1}] [\hat{K}(y_{T-1}) \hat{\Sigma}^{-1}] \cdots [\hat{K}(y_1) \hat{\Sigma}^{-1}] \hat{\mu} \\
&= [(\mu + \widehat{\Delta\mu})^\top (\Sigma + \widehat{\Delta\Sigma})^{-1}] [(K + \widehat{\Delta K})(y_T) (\Sigma + \widehat{\Delta\Sigma})^{-1}] \cdots [(K + \widehat{\Delta K})(y_1) (\Sigma + \widehat{\Delta\Sigma})^{-1}] (\mu + \widehat{\Delta\mu}).
\end{aligned} \tag{6}$$

Consider the matrix perturbation $(\Sigma + \widehat{\Delta\Sigma})^{-1} = \Sigma^{-1} - \Sigma^{-1} \widehat{\Delta\Sigma} \Sigma^{-1} + O(\|\widehat{\Delta\Sigma}\|^2)$, Here the matrix norm $\|\cdot\|$ can be any norm since all matrix norms have equivalent orders (Li, 2006). Also note that all items with $\widehat{\Delta}$ are $O_p(N^{-\frac{1}{2}})$. N is the number of i.i.d. triple (Y_1, Y_2, Y_3) for estimating $\hat{\mu}, \hat{\Sigma}, \hat{K}$. Note that N and T are not related, and that we work in the regime where T is fixed but $N \rightarrow \infty$. For example, $\hat{\mu} = \mu + \widehat{\Delta\mu} = \frac{1}{N} \sum_{i=1}^N Y_i \sim MVN(\mu, \frac{1}{N} Cov(Y))$. Similar analyses apply to $\hat{\Sigma}$ and \hat{K} can be similarly. So

$$\begin{aligned}
\widehat{\Delta\mu} &= [O_p(N^{-1/2})]^{(d)}; \\
\widehat{\Delta\Sigma} &= [O_p(N^{-1/2})]^{(d \times d)}; \\
\widehat{\Delta K} &= [O_p(N^{-1/2})]^{(d \times d \times d)},
\end{aligned}$$

where d is the dimension of Y_t . One application is $(\Sigma + \widehat{\Delta\Sigma})^{-1} = \Sigma^{-1} - \Sigma^{-1} \widehat{\Delta\Sigma} \Sigma^{-1} + O_p(N^{-1})$.

According to the previous two expansions, we could rewrite Eq 6. We could distribute

$$\begin{aligned}
& [(\mu + \widehat{\Delta\mu})^\top (\Sigma + \widehat{\Delta\Sigma})^{-1}] [(K + \widehat{\Delta K})(y_T) (\Sigma + \widehat{\Delta\Sigma})^{-1}] \cdots [(K + \widehat{\Delta K})(y_1) (\Sigma + \widehat{\Delta\Sigma})^{-1}] (\mu + \widehat{\Delta\mu}) \\
= & [(\mu + \widehat{\Delta\mu})^\top (\Sigma^{-1} - \Sigma^{-1} \widehat{\Delta\Sigma} \Sigma^{-1} + O_p(N^{-1}))] [(K + \widehat{\Delta K})(y_T) (\Sigma^{-1} - \Sigma^{-1} \widehat{\Delta\Sigma} \Sigma^{-1} + O_p(N^{-1}))] \cdots \\
& [(K + \widehat{\Delta K})(y_1) (\Sigma^{-1} - \Sigma^{-1} \widehat{\Delta\Sigma} \Sigma^{-1} + O_p(N^{-1}))] (\mu + \widehat{\Delta\mu}) \\
= & \mu^\top \Sigma^{-1} K(y_T) \Sigma^{-1} \cdots K(y_1) \Sigma^{-1} \mu + (v + \tilde{v})^\top \widehat{\Delta\mu} + \sum_{t=1}^T a_t^\top \widehat{\Delta K}(y_t) \tilde{a}_t - \sum_{t=0}^T b_t^\top \widehat{\Delta\Sigma} \tilde{b}_t + O_p(N^{-1}) \\
= & Pr(x_{1:T}) + (v + \tilde{v})^\top \widehat{\Delta\mu} + \sum_{t=1}^T a_t^\top \widehat{\Delta K}(y_t) \tilde{a}_t - \sum_{t=0}^T b_t^\top \widehat{\Delta\Sigma} \tilde{b}_t + O_p(N^{-1})
\end{aligned}$$

In the above, we first substitute $(\Sigma + \widehat{\Delta\Sigma})^{-1}$ by $\Sigma^{-1} - \Sigma^{-1} \widehat{\Delta\Sigma} \Sigma^{-1} + O_p(N^{-1})$. Then we distribute all multiplications. After distribution, there will be finite terms. We could categorize these forms into 3 categories according to different orders of convergence. The first category is the deterministic term without randomness. There is only one term in this category, $\mu^\top \Sigma^{-1} K(y_T) \Sigma^{-1} \cdots K(y_1) \Sigma^{-1} \mu$, which is $Pr(x_{1:T})$. The second category is the part that converges with order $O_p(N^{-1/2})$. This category involves all terms with one ' $\widehat{\Delta}$ ' term, i.e. one $\widehat{\Delta\mu}$, $\widehat{\Delta\Sigma}$ or $\widehat{\Delta K}$. This category is $(v + \tilde{v})^\top \widehat{\Delta\mu} + \sum_{t=1}^T a_t^\top \widehat{\Delta K}(y_t) \tilde{a}_t - \sum_{t=0}^T b_t^\top \widehat{\Delta\Sigma} \tilde{b}_t$. For simplicity of subsequent theorem proof, we simplify each term in the following way: for each ' $\widehat{\Delta}$ ' term, we denote the part in front of or behind them by $v, \tilde{v}, a_t, \tilde{a}_t, b_t, \tilde{b}_t$ as defined in this lemma. The third categories are all remaining terms. These terms are converging faster than or in the order of $O_p(N^{-1})$. There are finite terms in this category, so the summation of them is still $O_p(N^{-1})$.

□

Lemma 1 shows that how the estimated error propagates to the likelihood approximation. We can leverage the fact that our moment estimators have a central limit theorem (CLT) property to obtain the desired results in Theorem 1.

In the following theorem, we denote the outer product as \otimes , and define a “flattening” operator $\mathcal{F}(\cdot)$ for both matrices and 3-way tensors. For matrix $A_{d \times d}$,

$$\mathcal{F}(A) = [A^{(1,1)}, A^{(1,2)}, \dots, A^{(d,d)}]^\top;$$

For tensor $B_{d \times d \times d}$,

$$\mathcal{F}(B) = [B^{(1,1,1)}, B^{(1,1,2)}, \dots, B^{(1,1,d)}, B^{(1,2,1)}, B^{(1,2,2)}, \dots, B^{(1,2,d)}, \dots, B^{(1,d,d)}, \dots, B^{(d,d,d)}]^\top$$

We now state and prove our main theorem.

Theorem 1.

$$\sqrt{N}(\widehat{Pr}(x_{1:T}) - Pr(x_{1:T})) \xrightarrow{d} MVN \left(0, \beta^\top Cov \left(\begin{bmatrix} Y_1 \\ \mathcal{F}(Y_2 \otimes Y_1) \\ \mathcal{F}(Y_3 \otimes Y_1 \otimes Y_2) \end{bmatrix} \right) \beta \right),$$

where

$$\beta = \left[(v + \tilde{v})^\top; - \left(\sum_{t=0}^T \mathcal{F}(b_t \otimes \tilde{b}_t) \right)^\top; \left(\sum_{t=1}^T \mathcal{F}(a_t \otimes \tilde{a}_t \otimes y_t) \right)^\top \right]^\top$$

and $v, \tilde{v}, a_t, \tilde{a}_t, b_t, \tilde{b}_t$ are defined as in Lemma 1.

Proof (Theorem 1). We flatten $\widehat{\Delta\Sigma}$ and $\widehat{\Delta K}$ as

$$\begin{aligned} \mathcal{F}(\widehat{\Delta\Sigma}) &= [\widehat{\Delta\Sigma}^{(1,1)}, \widehat{\Delta\Sigma}^{(1,2)}, \dots, \widehat{\Delta\Sigma}^{(d,d)}]^\top, \\ \mathcal{F}(\widehat{\Delta K}) &= [\widehat{\Delta K}^{(1,1,1)}, \widehat{\Delta K}^{(1,1,2)}, \dots, \widehat{\Delta K}^{(d,d,d)}]^\top. \end{aligned}$$

Rewriting $a_t^\top \widehat{\Delta K}(y_t) \tilde{a}_t$ and $b_t^\top \widehat{\Delta\Sigma} \tilde{b}_t$ in Eq 6 as

$$\begin{aligned} a_t^\top \widehat{\Delta K}(y_t) \tilde{a}_t &= \mathcal{F}(a_t \otimes \tilde{a}_t \otimes y_t)^\top \cdot \mathcal{F}(\widehat{\Delta K}), \\ b_t^\top \widehat{\Delta\Sigma} \tilde{b}_t &= \mathcal{F}(b_t \otimes \tilde{b}_t)^\top \cdot \mathcal{F}(\widehat{\Delta\Sigma}), \end{aligned}$$

we have

$$\begin{aligned} &\widehat{Pr}(x_{1:T}) - Pr(x_{1:T}) - O_p(N^{-1}) \\ &= \left[(v + \tilde{v})^\top; - \left(\sum_{t=0}^T \mathcal{F}(b_t \otimes \tilde{b}_t) \right)^\top; \left(\sum_{t=1}^T \mathcal{F}(a_t \otimes \tilde{a}_t \otimes y_t) \right)^\top \right] \cdot \begin{bmatrix} \widehat{\Delta\mu} \\ \mathcal{F}(\widehat{\Delta\Sigma}) \\ \mathcal{F}(\widehat{\Delta K}) \end{bmatrix} \\ &= \beta^\top \cdot \widehat{\Delta\theta}. \end{aligned}$$

Since the central limit theorem applies separately to $\widehat{\Delta\mu}, \widehat{\Delta\Sigma}, \widehat{\Delta K}$, then

$$\sqrt{N}\widehat{\Delta\theta} = \sqrt{N} \begin{bmatrix} \frac{1}{N} \sum_{i=1}^N Y_{i,1} - \mu \\ \mathcal{F}\left(\frac{1}{N} \sum_{i=1}^N Y_{i,2} \otimes Y_{i,1} - \Sigma\right) \\ \mathcal{F}\left(\frac{1}{N} \sum_{i=1}^N Y_{i,3} \otimes Y_{i,1} \otimes Y_{i,2} - K\right) \end{bmatrix} \xrightarrow{d} MVN \left(\vec{0}, Cov \left(\begin{bmatrix} Y_1 \\ \mathcal{F}(Y_2 \otimes Y_1) \\ \mathcal{F}(Y_3 \otimes Y_1 \otimes Y_2) \end{bmatrix} \right) \right)$$

. Therefore,

$$\sqrt{N}(\widehat{Pr}(x_{1:T}) - Pr(x_{1:T})) \xrightarrow{d} MVN \left(0, \beta^\top Cov \left(\begin{bmatrix} Y_1 \\ \mathcal{F}(Y_2 \otimes Y_1) \\ \mathcal{F}(Y_3 \otimes Y_1 \otimes Y_2) \end{bmatrix} \right) \beta \right).$$

□

3 Projected SHMM

3.1 Motivation for Adding Projection

In the Baum-Welch algorithm (Baum et al., 1970), when we make a prediction, we are effectively predicting the belief probabilities, or weights, for each underlying cluster. Denote the predicted weight vector at time t as \hat{w}_t . Then the prediction can be expressed as a weighted combination of cluster means $\hat{y}_t = M\hat{w}_t$ where $\|\hat{w}_t\|_1 = 1$. The weights are explicitly guaranteed to be non-negative and sum to 1 during forward propagation in the Baum-Welch algorithm, which is consistent with their physical meaning. However, these two constraints are not explicitly implemented in spectral estimation since SHMM doesn't estimate the weights directly. Therefore, SHMM can sometimes give predictions which are far away from the polyhedron spanned by the cluster means. In order to solve this problem, we propose the projected SHMM, where projection serves to regularize the predictions to be within a reasonable range.

3.2 Projection-onto-polyhedron and Projection-onto-Simplex SHMM

There are two ways to achieve projection for our problem: projection-onto-polyhedron and projection-onto-simplex. Projection-onto-polyhedron stems directly from the motivation for using projections but suffers from high computational cost. To obtain a better computational performance, we propose projection-onto-simplex as an alternative.

3.2.1 Projection-onto-Polyhedron

Projection-onto-polyhedron SHMM first predicts $\hat{y}_t^{(SHMM)}$ through the standard SHMM and then projects it on to the polyhedron with vertices \widehat{M} . In other words, we find the point on the

polyhedron spanned by \widehat{M} that is nearest to the predicted $\hat{y}_t^{(SHMM)}$. We can use any distance to define “nearest point” but in our exposition we work with Euclidean distance. Mathematically, we substitute the recursive forecasting in Eq 3 with

$$\begin{aligned}\hat{y}_t^{(SHMM)} &= \frac{C(y_{t-1})\hat{y}_{t-1}}{c_\infty^\top C(y_{t-1})\hat{y}_{t-1}}; \\ \hat{y}_t &= \arg \min_{y \in Poly(\widehat{M})} d(y, \hat{y}_t^{(SHMM)}),\end{aligned}\tag{7}$$

where $d(\cdot, \cdot)$ is the distance function (such as Euclidean distance), and

$$Poly(\widehat{M}) = \{y = \widehat{M}w \mid w \text{ is on the simplex}\}$$

is the polyhedron with vertices \widehat{M} . This results in a convex optimization problem if the distance is convex, which is true for general distance functions such as Euclidean distance. We can solve this using standard convex optimization methods such as the Newton-Raphson algorithm (Boyd et al., 2004), with variants allowing linear constraints such as the log-barrier methods (Frisch, 1955). To the best of our knowledge, there is no dedicated algorithm for solving projection-onto-polyhedron, and unfortunately finding a fast solution seems to be challenging. The approach we take is to write the loss function of the constrained problem as the loss function with an indicator function, and use the log-barrier method to approximate the linear constraints through log-barrier functions. We then use the Newton-Raphson algorithm to optimize this approximated loss function, iteratively relaxing the approximation and solving it again until convergence. Note that this optimization needs to be done for every time step. This implies a trade-off between the accuracy of the approximation and optimization. Recall that we turn to SHMM because it is faster than the Baum-Welch algorithm, so any modification should not slow down the computation too much, otherwise this mitigates one of its strong advantages.

3.2.2 Projection-onto-Simplex

To obtain higher efficiency in computation, we propose a second projection regularization method: projection-onto-simplex. It leverages an algorithm that allows us to calculate the projection with time complexity $\mathcal{O}(d \log(d))$ (Wang and Carreira-Perpinán, 2013). To avoid projection onto a polyhedron, we leverage the fact that $\hat{y}_t = \widehat{M}\hat{w}_t$ and optimize over \hat{w}_t which lies on the simplex.

Algorithm 1: Projection-onto-simplex (Wang and Carreira-Perpinán, 2013).

Input : $u = [u_1, u_2, \dots, u_d]^\top$

Sort u into z : $z_1 \geq z_2 \dots \geq z_d$;

Find $\rho = \max\{1 \leq i \leq d : z_i + \frac{1}{i}(1 - \sum_{j=1}^i z_j) > 0\}$;

Define $\lambda = \frac{1}{\rho}(1 - \sum_{j=1}^{\rho} z_j)$;

Solve $u^{(proj)}$, s.t. $u_i^{(proj)} = \max(u_i + \lambda, 0)$, $i = 1, \dots, d$;

Output: $u^{(proj)}$

Mathematically, the optimization problem becomes

$$\hat{w}_t = \arg \min_{w \in Simplex} \|w - \widehat{M}^{-1} \hat{g}_t^{(SHMM)}\|_2^2. \quad (8)$$

This solution is not equivalent to solution from the projection-onto-polyhedron, because $d(a, b) \neq d(Aa, Ab)$ in general. But the solution set is the same, i.e. the predictions are both guaranteed to be constrained to the polyhedron. The solution of Eq 8 can be obtained through a closed-form solution provided in Algorithm 1, which avoids iterations during convex optimization which yields fast estimation. Figure 3 gives a graphical demonstration for the projection-onto-polyhedron and projection-onto-simplex methods.

The full projected SHMM algorithm is shown in Algorithm 2. In Algorithm 2, Steps 1-3 are identical to the standard SHMM. Steps 4-5 estimate \hat{M} by Gaussian Mixture Models (GMM) (McLachlan and Basford, 1988), calculate the weight processes $\{w_t\}$, and apply SHMM on the weight process. Step 6 applies projection-onto-simplex on the recursive forecasting. Step 7 projects the data back into the original space.

3.3 Choice of Hyperparameters and Variants of PSHMM

In this part, we first discuss the choice of hyperparameters and then we talk about variations of PSHMM.

3.3.1 The choice of hyperparameter d

d is the dimensionality of the projection space. From the theory of SHMM, d should equal the number of states in the HMM. Our simulations show that when d is chosen to be equal to the

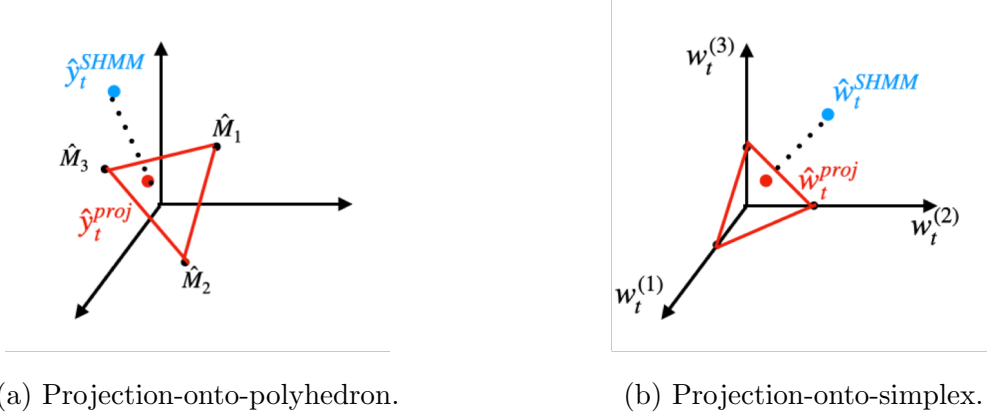


Figure 3: The left figure shows the projection-onto-polyhedron step, and the right one is the projection-onto-simplex step. In both two methods, we project the predicted values (blue points) into the constrained regions (areas with red boundary), polyhedron (left) or simplex (right).

Algorithm 2: Projection-onto-simplex SHMM.

Input : $\{x_t\}$, where $t = 1, \dots, T$

Output: \hat{x}_{T+1}

Step 1: Compute $\hat{E}[x_{t+1} \otimes x_t] = \frac{1}{T-2} \sum_{i=1}^{T-2} x_{t+1} x_t^\top$;

Step 2: Obtain \hat{U} by extracting the first k left eigenvectors of $\hat{E}[x_{t+1} \otimes x_t]$;

Step 3: Reduce dimensionality $\hat{y}_t = \hat{U}^\top x_t$;

Step 4: Estimate cluster mean by GMM, and obtain \hat{M} , where each column is the mean vector of each cluster. Then the weight vector is $w_t = \hat{M}^{-1} y_t$ for $t = 1, \dots, T$;

Step 5: Calculate $\hat{\mu} = \frac{1}{T} \sum_{t=1}^\top w_t$, $\hat{\Sigma} = \frac{1}{T-1} \sum_{t=1}^{T-1} w_{t+1} w_t^\top$, and

$\hat{K} = \frac{1}{T-2} \sum_{t=1}^{T-2} w_{t+2} \otimes w_t \otimes w_{t+1}$. Set $\hat{c}_1 = \hat{\mu}$, $\hat{c}_\infty^\top = c_1^\top \hat{\Sigma}^{-1}$, and $\hat{C}(w_t) = \hat{K}(w_t) \hat{\Sigma}^{-1}$;

Step 6: Recursive prediction with projection-onto-simplex $\hat{w}_t = Proj\left(\frac{\hat{C}(w_{t-1}) \hat{w}_{t-1}}{\hat{c}_\infty^\top \hat{C}(w_{t-1}) \hat{w}_{t-1}}\right)$ for $t = 2, \dots, T+1$ where $Proj(a) = \arg \min_{w \in Simplex} \|w - a\|_2^2$ can be solved by Algorithm 1, and set $\hat{y}_1 = \hat{c}_1$;

Step 7: $\hat{x}_{T+1} = \hat{U} \hat{y}_{T+1} = \hat{U} \hat{M} \hat{w}_{T+1}$;

underlying true number of states, the estimation and prediction will perform better than at other values of d . However, the number of hidden states is usually unknown. In practice, we can either choose d using prior knowledge or tune it if we don't have a strong prior belief.

3.3.2 Calculation of U matrix Under Extremely High-Dimensional Data: Unigram or Bigram Randomized SVD

The projection matrix U is constructed by the first d left singular vectors from the singular value decomposition (SVD) (Eckart and Young, 1936) of the bigram covariance matrix $\hat{\Sigma} = \hat{E}[X_2 \otimes X_1]$. This encodes the transition information and will eliminate the in-cluster covariance structure. However, this is not the only acceptable projection. We could also estimate U through an SVD of $\hat{E}[X_1 \otimes X_1]$. This result will encode covariance structure along with the cluster mean information. In most cases we suggest using the bigram matrix.

A point worth mentioning is that for extremely high-dimensional cases, we can leverage a fast approximation algorithm for computing \hat{U} . The algorithm is based on randomized SVD (Halko et al., 2011). In addition, when computing the SVD of the bigram matrix, we need to avoid computing the covariance matrix $\hat{E}[x_{t+1} \otimes x_t]$. The standard algorithm for the SVD requires time complexity $\mathcal{O}(Tp^2 + p^3)$, where T and p are the sample size and dimensionality of the dataset. For the high-dimensional cases where $p \gg d$, the randomized SVD has time complexity $\mathcal{O}(pT \log(d) + (p + T)d^2)$. In this case, the bottleneck is the computation of $\hat{E}[x_{t+1} \otimes x_t]$, whose time complexity is $\mathcal{O}(Tp^2)$.

Note that $\hat{E}[x_{t+1} \otimes x_t] = \frac{1}{T-2} \sum_{i=1}^{T-2} x_{t+1} x_i^\top = \frac{1}{T-2} X_2^\top X_1$, where $X_2 = [x_2, \dots, x_T]^\top$ and $X_1 = [x_1, \dots, x_{T-1}]^\top$. We can take the randomized SVD of X_1 and X_2 separately to obtain two rank- \tilde{d} decompositions with $d \leq \tilde{d} \ll p$: $X_1 \approx U_1 \Sigma_1 V_1^\top$, $X_2 \approx U_2 \Sigma_2 V_2^\top$. Then $X_2^\top X_1 = V_1 (\Sigma_1 U_1^\top U_2 \Sigma_2) V_2^\top$. $(\Sigma_1 U_1^\top U_2 \Sigma_2)$ is a $\tilde{d} \times \tilde{d}$ matrix, and computing it is much faster than computing $\hat{E}[x_{t+1} \otimes x_t]$. We could perform SVD on this matrix to get $\Sigma_1 U_1^\top U_2 \Sigma_2 = \tilde{U} \tilde{\Sigma} \tilde{V}^\top$. So $\hat{E}[x_{t+1} \otimes x_t] \approx (V_1 \tilde{U}) (\frac{1}{T-2} \tilde{\Sigma}) (V_2 \tilde{V})^\top$. Note that $V_1 \tilde{U}$ and $V_2 \tilde{V}$ are orthonormal matrices and $\frac{1}{T-2} \tilde{\Sigma}$ is a diagonal matrix, so this is the rank- \tilde{d} SVD of $\hat{E}[x_{t+1} \otimes x_t]$. The first d vectors of $V_1 \tilde{U}$ are the \hat{U} matrix we are to compute in Step 1 and 2 in Algorithm 2.

3.3.3 Projecting $\{w_t\}$ onto the Probability Space

Another advantage of PSHMM is that we can project X_t onto the probability space y whose i -th element is the probability that the original data point belongs to the i -th cluster $y_t^{(i)} = P(h = i | X_t)$. This probability is similar to the emission probability in Gaussian HMM but is now computed by GMM. To do this, we only need to substitute the Step 4 in Algorithm 2. We calculate w_t from

the probability of belonging to different components in the GMM instead of $\hat{M}^{-1}y_t$.

The advantage of this method is interpretation. In this model, w_t has a straightforward probabilistic meaning, i.e. the weight on different components for a given observation. The SHMM prediction is then on w_t , the weight process. In comparison, w_t in Algorithm 2 is calculated purely based on the moments. If we use the probability space, PSHMM is no longer a method only based on moments. It is a mix of moment-based and distribution-based methods.

4 Online Learning

4.1 Online Learning of SHMM and PSHMM

To adapt the SHMM and PSHMM models as we obtain more data, we first estimate the first, second and third moments based on a warm-up sequence $\{Y_t\}_{t=1}^{T_{warmup}}$:

$$\begin{aligned}\hat{\mu} &\leftarrow \frac{1}{T_{warmup}} \sum_{t=1}^{T_{warmup}} Y_t; \\ \hat{\Sigma} &\leftarrow \frac{1}{T_{warmup} - 1} \sum_{t=1}^{T_{warmup}-1} Y_{t+1} \otimes Y_t; \\ \hat{K} &\leftarrow \frac{1}{T_{warmup} - 2} \sum_{t=1}^{T_{warmup}-2} Y_{t+2} \otimes Y_t \otimes Y_{t+1}; \\ T &\leftarrow T_{warmup}.\end{aligned}$$

When we obtain new data Y_{T+1} , we update our moments as follows:

$$\begin{aligned}\hat{\mu} &\leftarrow \frac{T \cdot \hat{\mu} + Y_{T+1}}{T + 1}; \\ \hat{\Sigma} &\leftarrow \frac{(T - 1) \cdot \hat{\Sigma} + Y_{T+1} \otimes Y_T}{T}; \\ \hat{K} &\leftarrow \frac{(T - 2) \cdot \hat{K} + Y_{T+1} \otimes Y_{T-1} \otimes Y_T}{T - 1}; \\ T &\leftarrow T + 1.\end{aligned}\tag{9}$$

The above updating rule works for both SHMM and PSHMM. The pseudo code for online learning PSHMM is shown in Algorithm 3.

Algorithm 3: Online learning Projection-onto-simplex SHMM.

Input : $\{x_t\}_{t=1, \dots, T}$, the warm-up length T_{warmup}

Output: $\{\hat{x}_t\}_{t=T_{warmup}+1}^{T+1}$ yielded sequentially.

Step 1: Compute $\hat{E}[x_{t+1} \otimes x_t]^{(warmup)} = \frac{1}{T_{warmup}-2} \sum_{i=1}^{T_{warmup}-2} x_{t+1} x_t^\top$;

Step 2: Obtain \hat{U} by extracting the first k left eigenvectors of $\hat{E}[x_{t+1} \otimes x_t]^{(warmup)}$;

Step 3: Reduce dimensionality $\hat{y}_t = \hat{U}^\top x_t$ for $t = 1, \dots, T_{warmup}$;

Step 4: Estimate cluster mean by GMM by data $\{\hat{y}_t\}_{t=1}^{T_{warmup}}$, and obtain \hat{M} , where each column is the mean vector of each cluster. Then the weight vector is $w_t = \hat{M}^{-1} y_t$ for $t = 1, \dots, T_{warmup}$;

Step 5: Calculate $\hat{\mu}$, $\hat{\Sigma}$, \hat{K} , \hat{c}_1 , \hat{c}_∞^\top and $\hat{C}(\cdot)$ as described in Step 5 of Algorithm 2;

Step 6: Recursive prediction with projection-onto-simplex \hat{w}_t for $t = 1, \dots, T_{warmup} + 1$ as described in Step 6 of Algorithm 2. Yield $\hat{x}_{T_{warmup}+1} = \hat{U} \hat{M} \hat{w}_{T_{warmup}+1}$;

Step 7 (online learning and prediction):

for $t \leftarrow T_{warmup} + 1$ **to** T **do**

$w_t = \hat{M}^{-1} \hat{U}^\top x_t$;

Update $\hat{\mu}$, $\hat{\Sigma}$ and \hat{K} according to Eq 9;

Predict \hat{w}_{t+1} by $\hat{w}_{t+1} = Proj\left(\frac{\hat{C}(w_t) \hat{w}_t}{\hat{c}_\infty^\top \hat{C}(w_t) \hat{w}_t}\right)$, where $\hat{C}(\cdot)$ and \hat{c}_∞^\top are based on updated $\hat{\mu}$, $\hat{\Sigma}$ and \hat{K} , and $Proj(\cdot)$ is solved by Algorithm 1;

Yield $\hat{x}_{t+1} = \hat{U} \hat{M} \hat{w}_{t+1}$;

end

For updating GMM for PSHMM To update the first, second and third order moments of w_t , we could just replace Y with w on above formulas. The only consideration is whether to update GMM or not. There are multiple ways of updating GMM. We recommend to update it without changing the cluster, for example, we classify a new input into different clusters and update each cluster's mean and covariance. We don't suggest the online learning algorithm of GMM that allows adding or removing clusters. The number of clusters is pre-specified as it should be equal to the number of states in HMM and the dimensionality of space y . The addition of deletion of a cluster in GMM might fundamentally change this requirement. In practice, we found that PSHMM works well without updating GMM.

4.2 Online Learning of SHMM Class with Forgetfulness

When dealing with instationary data, it might help if we add a forgetting mechanism on parameter estimation. Particularly, we could add a forgetting mechanism on the moment estimation. It is equivalent to the exponentially weighted average. First specify a decay factor γ that the information is forgotten by the rate $1 - \gamma$, then the updating rule is

$$\begin{aligned}
 \hat{\mu} &\leftarrow \frac{(1 - \gamma)\tilde{T}\hat{\mu} + Y_{T+1}}{(1 - \gamma)\tilde{T} + 1}; \\
 \hat{\Sigma} &\leftarrow \frac{(1 - \gamma)\tilde{T}\hat{\Sigma} + Y_{T+1} \otimes Y_T}{(1 - \gamma)\tilde{T} + 1}; \\
 \hat{K} &\leftarrow \frac{(1 - \gamma)\tilde{T}\hat{K} + Y_{T+1} \otimes Y_{T-1} \otimes Y_T}{(1 - \gamma)\tilde{T} + 1}; \\
 \tilde{T} &\leftarrow \tilde{T} \cdot (1 - \gamma) + 1.
 \end{aligned} \tag{10}$$

Here $\tilde{T} = \sum_{i=1}^T (1 - \gamma)^{i-1}$ serve as an effective sample size. This strategy is equivalent to calculating the exponentially weighted moving average that

$$\hat{\mu} = \frac{\sum_{t=1}^T (1 - \gamma)^{T-t} Y_t}{\sum_{t=1}^T (1 - \gamma)^{T-t}}; \hat{\Sigma} = \frac{\sum_{t=2}^T (1 - \gamma)^{T-t} Y_t \otimes Y_{t-1}}{\sum_{t=2}^T (1 - \gamma)^{T-t}}; \hat{K} = \frac{\sum_{t=3}^T (1 - \gamma)^{T-t} Y_t \otimes Y_{t-2} \otimes Y_{t-1}}{\sum_{t=3}^T (1 - \gamma)^{T-t}}. \tag{11}$$

5 Simulations

5.1 Test Robustness under Different Signal-Noise Ratio, Mis-specified Models and Heavy-Tailed Data

5.1.1 Experiment setting

We generated 100-dimensional data with length 10000 for training data and 100 for testing data under different settings, and used SHMM and PSHMM with recursive prediction for time series forecasting. We repeated each simulation setup 100 times, calculated R^2 for each repeat, and computed an average R^2 over all repeats. The results below show this averaged R^2 . We tested 3 variants of the PSHMM: projection onto polyhedron, projection onto simplex, and projection onto simplex with online learning. The online learning variant of PSHMM used 1000 training samples for the initial estimate (warm-up), and incorporated the remaining 9000 training samples

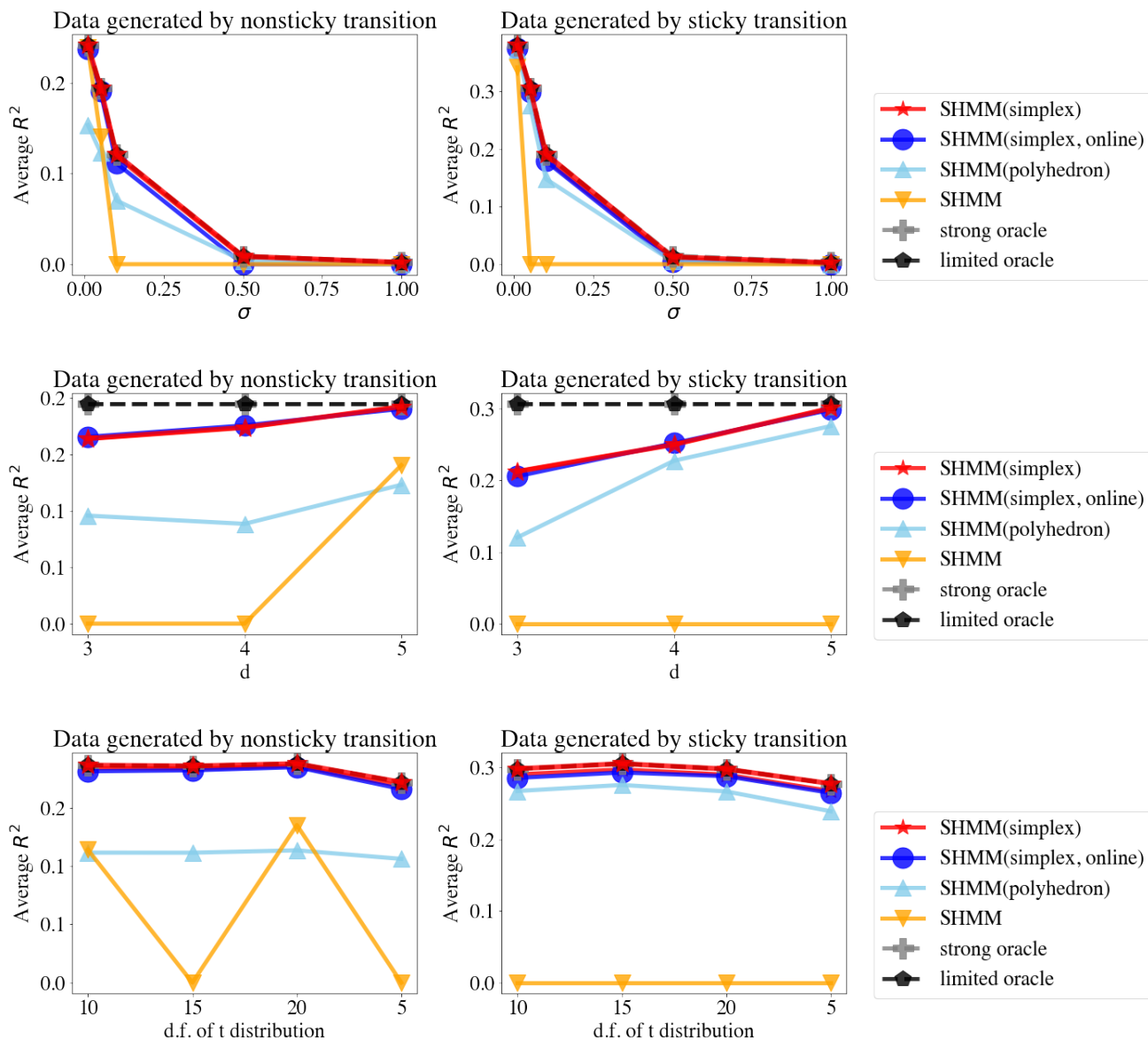


Figure 4: These subfigures show the simulation results for experiment settings in Section 5.1.1. The left column shows the results of sticky transition, and the right column shows the nonsticky transition. The first row is the results for 5-state GHMM with different σ , the second row is the results for inferring 5-state GHMM of $\sigma = 0.05$ with different d , and the last row is the results for 5-state t-distribution HMM of $\sigma = 0.05$ with different degrees of freedom for t-distribution. In each subfigure, the y-axis is R^2 and different curves are for different methods. For $R^2 < 0$, we plot 0 instead of the negative for plotting purpose. See supplementary for detailed results.

using online updates. In our simulations, online training for PSHMM differs from offline training for two reasons. First, the estimation of \hat{U} and \hat{M} are based only on the warm-up set for online learning (as is the case for the online version of SHMM), and the entire training set for offline learning. Second, during the training period, for PSHMM, the updated moments are based on the recursive predictions of \hat{w}_t , which are themselves based on the weights $\{w_s\}_{s=1}^{t-1}$. For offline learning of PSHMM in contrast, the weights used to calculate the moments are based on the GMM estimates from the entire training dataset. For each state, we assumed the emission distribution has a one-hot mean vector and diagonal covariance matrix, that the mean vector of the i -th state is $[1\{i = j\}]_{j=1}^p$ where $1\{\cdot\}$ is the indicator function. We tested those two methods under two types of transition matrix, three different signal-noise ratios and different distributions as below:

- Transition matrix:
 - Sticky transition matrix: diagonal elements are 0.6, off-diagonal elements are $\frac{0.4}{S-1}$, where S is the hyperparameter that tell how many clusters that generated the data;
 - Non-sticky transition matrix: diagonal elements are 0.4, off-diagonal elements are $\frac{0.6}{S-1}$.
- Signal-noise ratio: The covariance matrix of each cluster is: $\sigma^2 I_p$, where p is the dimension of the space, $\sigma = 0.01, 0.05, 0.1, 0.5, 1.0$.
- Data generated from:
 - Gaussian distribution: generate according to mean vector and covariance matrix;
 - t distribution: generate standard a random vector of *i.i.d.* t_5, t_{10}, t_{15} and t_{20} distribution first, and then multiply by covariance matrix and shifted by mean vector.

For each setting, we also showed the oracle R^2 . Strong oracle is to assume we know all parameters and the hidden states before the time stamp to predict. Limited oracle is to assume we know all parameters but don't know the hidden states.

5.1.2 Simulation Results

Figure 4 shows the simulation results. We see that adding projections greatly improved R^2 , nearly achieving performance of the oracle in some settings. The top row shows that in both high or

low signal-noise ratio case, PSHMM works well. The middle row shows that PSHMM is robust and outperforms SHMM when the model is mis-specified, for example, when the underlying data contains 5 states but we choose to reduce the dimensions to 3 or 4. The last row shows that PSHMM is more robust and has a better R^2 than SHMM with heavy-tailed data such as data generated by a t distribution. For $R^2 < 0$ in all these figures, we plot 0 instead of the negative for plotting purpose. See supplementary tables for detailed results. Negative R^2 occurs only for SHMM, implying that it is not stable. Overall, while SHMM often performs well, it is not robust, and PSHMM provides a suitable solution.

In all simulation settings, SHMM tends to give poor predictions except in non-sticky and high signal-to-noise ratio settings. PSHMM is more robust against noise and mis-specified models. Among the PSHMM variants, projection-onto-simplex outperforms projection-onto-polyhedron. The reason is that the projection-onto-simplex has a dedicated optimization algorithm that guarantees the optimal solution in the projection step. In contrast, projection-onto-polyhedron uses the log-barrier method, which is a general purpose optimization algorithm and does not guarantee the optimality of the solution. Since projection-onto-polyhedron also has a higher computational time, we recommend using projection-onto-simplex. Finally, for projection-onto-simplex, we see that online and offline estimation perform similarly in most settings, and thus online learning does not lose too much power compared with offline learning.

5.2 Test Computational Time

Experiment setting We used a similar experimental setting from Section 5.1.1. We simulated 100-dimensional, 3-state GHMM data with $\sigma = 0.05$ and of length 2000. We use the first half for warm-up and test computational time on the last 1000 time steps. We tested both E-M algorithm and SHMM. For SHMM, we tested under both online and offline learning regimes. We computed the total running time in seconds. The implementation is done in python with packages Numpy (Harris et al., 2020), Scipy (Virtanen et al., 2020) and scikit-learn (Pedregosa et al., 2011) without multithreading. Note that this was not the procedure from 5.1, and the whole process is repeated 30 times, and the computational time is the average of each time.

Results Table 1 shows the computational time. First, online learning substantially reduces the computational cost. For the offline learning methods, projection-onto-simplex SHMM performs similarly with SHMM, and projection-onto-polyhedron is much slower. In fact, the offline version of projection-onto-polyhedron is slow even compared to the the Baum-Welch algorithm. However, the online learning variant of projection-onto-polyhedron is much faster than the Baum-Welch algorithm. Taking both the computational time and prediction accuracy into consideration, online and offline projection-onto-simplex SHMM are the best choice among these methods.

Method	Offline/online	Computational time (sec)
EM (Baum-Welch)	-	2134
SHMM	offline	304
SHMM	online	0.5
PSHMM (simplex)	offline	521
PSHMM (simplex)	online	0.7
PSHMM (polyhedron)	offline	10178
PSHMM (polyhedron)	online	14

Table 1: Simulation results for comparing computational time among different methods.

6 Application: Backtesting on High Frequency Crypto-Currency Data

6.1 Data Description & Experiment Setting

To show the performance of our algorithm on real data, we used a crypto currency trading records dataset published by Binance (<https://data.binance.vision>), one of the largest Bitcoin exchanges in the world. We used the minute-level data, calculated the log return of each minute, then used the log returns as the input for the models. We set aside a test set from 2022-07-01 to 2022-12-31. For each day in the test set, we used the previous 30 days rolling period to train models, and made consecutive-minute recursive predictions over the testing day without updating model parameters. For currency, we chose Bitcoin, Ethereum, XRP, Cardano and Polygon. For

prediction, we used the HMM with E-M inference (HMM-EM), SHMM, PSHMM (simplex) and autoregressive (AR) (Box et al., 2015) and compared their performance. For HMM-EM, SHMM and PSHMM, we chose to use 4 latent states. This was motivated by the fact that there are 4 dominant types of log returns: combinations of large/small gain/loss. For AR, we chose lag-1.

Ultimately, we evaluate models based on the performance of a trading strategy. Translating predictions into a simulated trading strategy is straightforward, and proceeds as follows. If we forecast a positive return in the next minute, we buy the currency, and if we forecast a negative return, we short-sell the currency. We buy a fixed dollar amount of crypto-currency for each of the 5 currencies, hold it for one minute, and then sell it. We repeat this for every minute of the day, and calculate the return of that day as

$$R_m = \frac{1}{5} \sum_{i=1}^5 \sum_t \text{sign}(\widehat{Y}_{i,t}^{(m)}) Y_{i,t}^{(m)}$$

where $Y_{i,t}^{(m)}$ is the return for minute t of day m for currency i , $\widehat{Y}_{i,t}^{(m)}$ is its prediction, and $\text{sign}(a)$ is 1 if a is positive, -1 if a is negative, and 0 if $a = 0$. Over a period of M days, we obtain R_1, \dots, R_M and calculate the annualized return,

$$\text{Annualized return} = 365 \times \overline{R},$$

the Sharpe ratio (Sharpe, 1966)

$$\text{Sharpe ratio} = \frac{\sqrt{365} \times \overline{R}}{\widehat{\text{std}}(R)},$$

where \overline{R} and $\widehat{\text{std}}(R)$ is the sample mean and standard variance of these daily returns, and the maximum drawdown (Grossman and Zhou, 1993)

$$\text{Maximum drawdown} = \max_{m_2} \max_{m_1 < m_2} \left[\frac{\sum_{m=m_1}^{m_2} (-R_m)}{1 + \sum_{m=1}^{m_1} R_m} \right].$$

These three metrics are standard mechanisms for evaluating the success of a trading strategy in finance. The annualized return shows the ability of a strategy to generate revenue and is the most straightforward metric. Sharpe ratio is the risk-adjusted return, or the return earned per unit of risk, where the standard deviation of return is viewed as the risk. In general, we can increase both the return and risk by borrowing money or adding leverage, so Sharpe ratio is a better metric than annualized return because it is not affected by the leverage effect. Maximum drawdown is

the maximum percentage of decline from the peak. Since the financial data is leptokurtic, the maximum drawdown shows the outlier effect better than the Sharpe ratio which is purely based on the first and second order moments. A smaller maximum drawdown indicates that the method is less risky.

6.2 Results

Method	Sharpe Ratio	Annualized Return	Maximum drawdown
PSHMM	2.88	1012%	49%
SHMM	1.07	345%	90%
HMM-EM	0.89	197%	53%
AR	1.48	572%	114%

Table 2: Real-world application results: PSHMM, SHMM, HMM-EM and AR on crypto-currency trading.

From Table 2, we see that PSHMM outperforms all other benchmarks with the highest Sharpe ratio and annualized return, and the lowest maximum drawdown. PSHMM outperforms SHMM and SHMM outperforms HMM-EM. SHMM outperforms HMM-EM because the spectral learning doesn't suffer from the local minima problem of E-M algorithm. PSHMM outperforms SHMM because the projection-onto-simplex provides regularization.

The accumulated daily return is shown in Figure 5. We see that SHMM and HMM-EM are more stable but do not have as high returns as PSHMM and AR. This is reasonable as higher risk strategies tend to have higher returns. However, between PSHMM and AR, PSHMM has a higher return despite having a much smaller risk. The maximum drawdown of PSHMM is 49%. Considering the high volatility of the crypto currency market during the second half of 2022, this maximum drawdown is acceptable. On the other hand, the maximum drawdown of AR is 114%. In other words, the AR strategy would have gone bankrupt in this period. For computational purposes, the drawdown is allowed to be larger than 100% because we are always using a fixed amount of money to buy or sell, so effectively we are assuming an infinite pool of cash. Between PSHMM and SHMM, the only difference is from the projection-onto-simplex. We see that the maximum drawdown of PSHMM is only about half that of SHMM, showing that PSHMM takes

a relatively small risk, especially given that PSHMM has a much higher return than SHMM. Combining the higher return and lower risk, PSHMM performs substantially better than SHMM.

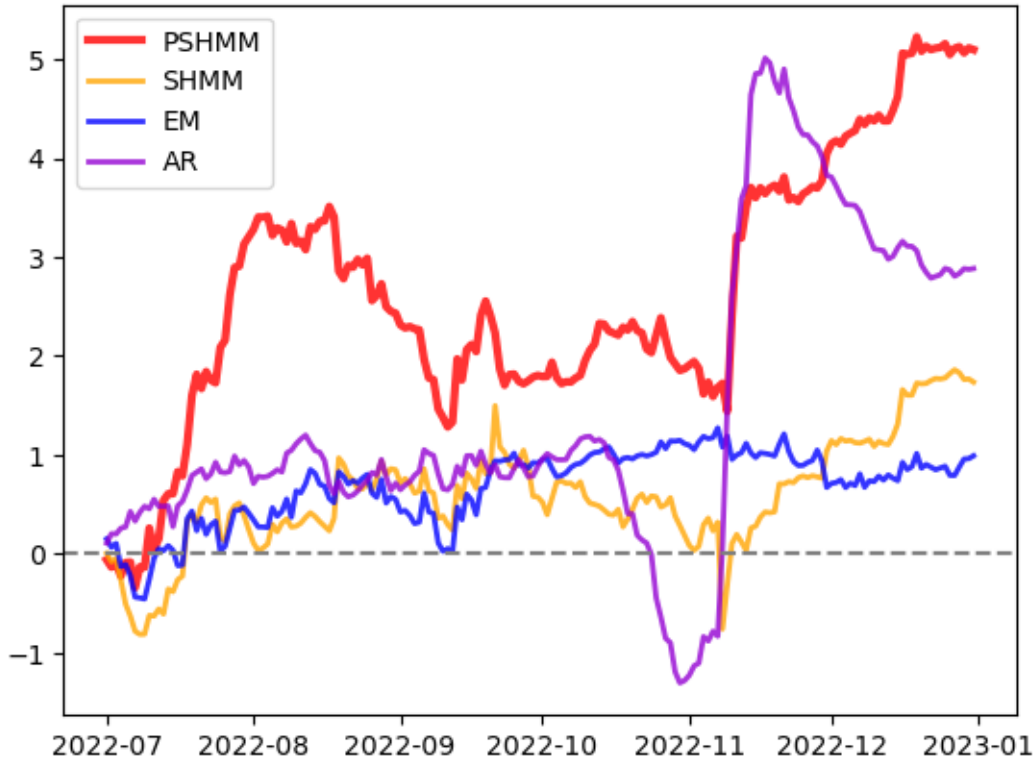


Figure 5: The accumulated return of bitcoin.

7 Discussion

Spectral estimation avoids being trapped in local minima. E-M (or the B-W algorithm) optimizes the likelihood function and is prone to local optima since the likelihood function is highly non-convex, while spectral estimation uses the MOM directly on the observations. Although trying different initializations could mitigate the problem with E-M, it cannot be entirely avoided. In other words, E-M algorithm doesn't guarantee the convergence to the true global optimum. Spectral estimation provides a framework for estimation which not only avoids non-convex optimization, but also has nice a theoretical property. The approximate error bound tells us that when the number of observations goes to infinity, the approximation error will go to zero. In this manuscript, we also provide the asymptotic distribution of this error.

Projection-onto-simplex serves as regularization. The standard SHMM can give poor predictions due to the accumulation and propagation of errors. Projection-onto-simplex pulls the prediction back to a reasonable range. This regularization is our primary methodological innovation, and importantly makes the SHMM well-suited for practical use. Although the simplex, estimated by the means from a GMM, can be biased, this simplex provides the most natural and reasonable choice for a projection space. We can think of this as a bias-variance tradeoff. When the data size is small, this regularization sacrifices bias to reduce variance.

Online learning can adapt to dynamic pattern and provide a faster learning. Finally, we provide an online learning strategy that allows the estimated moments to adapt over time, which is critical in several applications that can exhibit nonstationarity. Our online learning framework can be applied to both the standard SHMM and PSHMM. Importantly, online learning substantially reduces the computational costs compared to re-training the entire model prior to each new prediction.

SUPPLEMENTAL MATERIALS

Python-package for SHMM: Python-package *PSHMM* containing code to perform the SHMM and PSHMM described in the article. The package also contains all datasets used as examples in the article.

Detailed simulation results: Detailed simulation results behind figures in Section 5.

References

- Baum, L. E. and Petrie, T. (1966). Statistical inference for probabilistic functions of finite state markov chains. *The annals of mathematical statistics*, 37(6):1554–1563.
- Baum, L. E., Petrie, T., Soules, G., and Weiss, N. (1970). A maximization technique occurring in the statistical analysis of probabilistic functions of markov chains. *The annals of mathematical statistics*, 41(1):164–171.
- Box, G. E., Jenkins, G. M., Reinsel, G. C., and Ljung, G. M. (2015). *Time series analysis: forecasting and control*. John Wiley & Sons.
- Boyd, S., Boyd, S. P., and Vandenberghe, L. (2004). *Convex optimization*. Cambridge university press.
- Dempster, A. P., Laird, N. M., and Rubin, D. B. (1977). Maximum likelihood from incomplete data via the em algorithm. *Journal of the Royal Statistical Society: Series B (Methodological)*, 39(1):1–22.
- Eckart, C. and Young, G. (1936). The approximation of one matrix by another of lower rank. *Psychometrika*, 1(3):211–218.
- Frisch, K. (1955). The logarithmic potential method of convex programming. *Memorandum, University Institute of Economics, Oslo*, 5(6).
- Grossman, S. J. and Zhou, Z. (1993). Optimal investment strategies for controlling drawdowns. *Mathematical finance*, 3(3):241–276.

- Halko, N., Martinsson, P.-G., and Tropp, J. A. (2011). Finding structure with randomness: Probabilistic algorithms for constructing approximate matrix decompositions. *SIAM review*, 53(2):217–288.
- Harris, C. R., Millman, K. J., van der Walt, S. J., Gommers, R., Virtanen, P., Cournapeau, D., Wieser, E., Taylor, J., Berg, S., Smith, N. J., Kern, R., Picus, M., Hoyer, S., van Kerkwijk, M. H., Brett, M., Haldane, A., del Río, J. F., Wiebe, M., Peterson, P., Gérard-Marchant, P., Sheppard, K., Reddy, T., Weckesser, W., Abbasi, H., Gohlke, C., and Oliphant, T. E. (2020). Array programming with NumPy. *Nature*, 585(7825):357–362.
- Hsu, D., Kakade, S. M., and Zhang, T. (2012). A spectral algorithm for learning hidden markov models. *Journal of Computer and System Sciences*, 78(5):1460–1480.
- Knoll, B. C., Melton, G. B., Liu, H., Xu, H., and Pakhomov, S. V. (2016). Using synthetic clinical data to train an hmm-based pos tagger. In *2016 IEEE-EMBS International Conference on Biomedical and Health Informatics (BHI)*, pages 252–255. IEEE.
- Li, R.-C. (2006). Matrix perturbation theory. In *Handbook of linear algebra*, pages 15–1. Chapman and Hall/CRC.
- McLachlan, G. J. and Basford, K. E. (1988). *Mixture models: Inference and applications to clustering*, volume 38. M. Dekker New York.
- Pedregosa, F., Varoquaux, G., Gramfort, A., Michel, V., Thirion, B., Grisel, O., Blondel, M., Prettenhofer, P., Weiss, R., Dubourg, V., Vanderplas, J., Passos, A., Cournapeau, D., Brucher, M., Perrot, M., and Duchesnay, E. (2011). Scikit-learn: Machine learning in Python. *Journal of Machine Learning Research*, 12:2825–2830.
- Rodu, J. (2014). *Spectral estimation of hidden Markov models*. University of Pennsylvania.
- Rodu, J., Foster, D. P., Wu, W., and Ungar, L. H. (2013). Using regression for spectral estimation of hmms. In *International Conference on Statistical Language and Speech Processing*, pages 212–223. Springer.
- Sharpe, W. F. (1966). Mutual fund performance. *The Journal of business*, 39(1):119–138.

Virtanen, P., Gommers, R., Oliphant, T. E., Haberland, M., Reddy, T., Cournapeau, D., Burovski, E., Peterson, P., Weckesser, W., Bright, J., van der Walt, S. J., Brett, M., Wilson, J., Millman, K. J., Mayorov, N., Nelson, A. R. J., Jones, E., Kern, R., Larson, E., Carey, C. J., Polat, İ., Feng, Y., Moore, E. W., VanderPlas, J., Laxalde, D., Perktold, J., Cimrman, R., Henriksen, I., Quintero, E. A., Harris, C. R., Archibald, A. M., Ribeiro, A. H., Pedregosa, F., van Mulbregt, P., and SciPy 1.0 Contributors (2020). SciPy 1.0: Fundamental Algorithms for Scientific Computing in Python. *Nature Methods*, 17:261–272.

Wang, W. and Carreira-Perpinán, M. A. (2013). Projection onto the probability simplex: An efficient algorithm with a simple proof, and an application. *arXiv preprint arXiv:1309.1541*.